Liver 2000: 20: 487–490
Printed in Denmark . All rights reserved

Liver
ISSN 0106-9543

^{18}F-Fluorodeoxyglucose (FDG)-PET features of focal nodular hyperplasia (FNH) of the liver

Kurtaran A, Becherer A, Pfeffel F, Müller C, Traub T, Schmaljohann J, Kaserer K, Raderer M, Schima W, Dudczak R, Kletter K, Virgolini. ^{18}F-Fluorodeoxyglucose (FDG)-PET features of focal nodular hyperplasia (FNH) of the liver.
Liver 2000: 20: 487–490. © Munksgaard, 2000

Abstract: *Aim:* The aim of this paper is to describe the imaging pattern of focal nodular hyperplasia (FNH) by ^{18}F-fluorodeoxyglucose (18F-FDG) positron emission tomography (PET). *Methods:* Eight consecutive asymptomatic patients with histologic proof of FNH underwent 18F-FDG PET imaging. The lesions were found incidentally. The 18F-FDG PET imaging was performed with a dedicated PET tomograph after intravenous injection of 300–370 MBq 18F-FDG. The 18F-FDG accumulation in the lesions was (semi)quantified by calculating the standardized uptake value (SUV) and SUV has been corrected for the lean body mass (LBM). Eight patients with liver metastases spread from melanoma (n=2) and colorectal carcinoma (n=6) served as controls. The size of the FNH lesions and of the control group ranged from 2.0 to 8.5 cm (mean 4.83 cm±2.37) and from 1.5 to 6 cm (mean 3.28±1.52), respectively. *Results:* While in malignant liver lesions the accumulation of 18F-FDG was significantly increased, all FNH lesions showed normal or even decreased accumulation of 18F-FDG. In FNH lesions, SUV ranged between 1.5 and 2.6 (mean 2.12±0.38), whereas all liver metastases showed an increased SUV ranging between 6.20 and 16.00 (mean 10.07±3.79). The SUV corrected for LMB (SUV_{LBM}) was similar to the SUV and ranged between 0.9 and 2.2 (mean 1.81±0.41) for FNH and between 5.9 and 16.3 (mean 9.15±4.03), respectively. *Conclusion:* In contrast to liver metastases, there is no increased glucose metabolism in FNH *in vivo*. The imaging feature of FNH by 18F-FDG-PET imaging is not specific for FNH; however, it may be helpful to differentiate FNH from liver metastases in cancer patients if radiological methods are not diagnostic.

Amir Kurtaran[1], Alexander Becherer[1], Franz Pfeffel[2], Christian Müller[2], Tatjana Traub[1], Jörn Schmaljohann[1], Klaus Kaserer[3], Markus Raderer[2], Wolfgang Schima[4], Robert Dudczak[1], Kurt Kletter[1] and Irene Virgolini[1]

Departments of [1]Nuclear Medicine, [2]Internal Medicine, [3]Pathology, and [4]Radiology, University of Vienna, Vienna, Austria

Key words: hepatic focal nodular hyperplasia (FNH) – ^{18}F-fluorodeoxyglucose (18F-FDG) – positron emission tomography (PET)

A. Kurtaran, M.D., Department of Nuclear Medicine, University of Vienna, Währinger Gürtel 18–20, A-1090 Vienna, Austria.
Tel. and Fax: +43 1 40400 7835.
e-mail: amir.kurtaran@akh-wien.ac.at

Received 19 January, accepted 28 June 2000

Focal nodular hyperplasia (FNH) is a benign hepatic tumor usually discovered incidentally. The lesions are usually asymptomatic and occur mostly in females. In contrast to malignant liver lesions, FNH should be managed conservatively. A large number of imaging modalities have been used to diagnose FNH with variable success. Ultrasonography (US) can only be considered as a screening technique, since the appearance of FNH by US is non-specific. FNH may appear hyperdense or hypodense on computed tomography (CT) and a definite diagnosis of FNH may be challenging, especially if the lesions are small-sized (1, 2). Contrast-enhanced MRI is the best imaging procedure in the diagnosis of FNH if typical features of FNH are present (1). Nuclear medicine procedures such as ^{99m}Tc-sulfur colloid scintigraphy (^{99m}Tc-SC) and trimethyl bromo-imino-diacetic acid (TBIDA) and hepatocyte-specific receptor ligand ^{99m}Tc-galactosyl-neoglycoalbumin are other means of diagnosing FNH which have met with variable success (3–6).

PET is a new imaging method that has been successfully applied to image malignant tumors. While a large number of studies has been published in the last years about the usefulness of 18F-FDG PET in a variety of malignant diseases, the glucose metabolism of FNH *in vivo* has not been

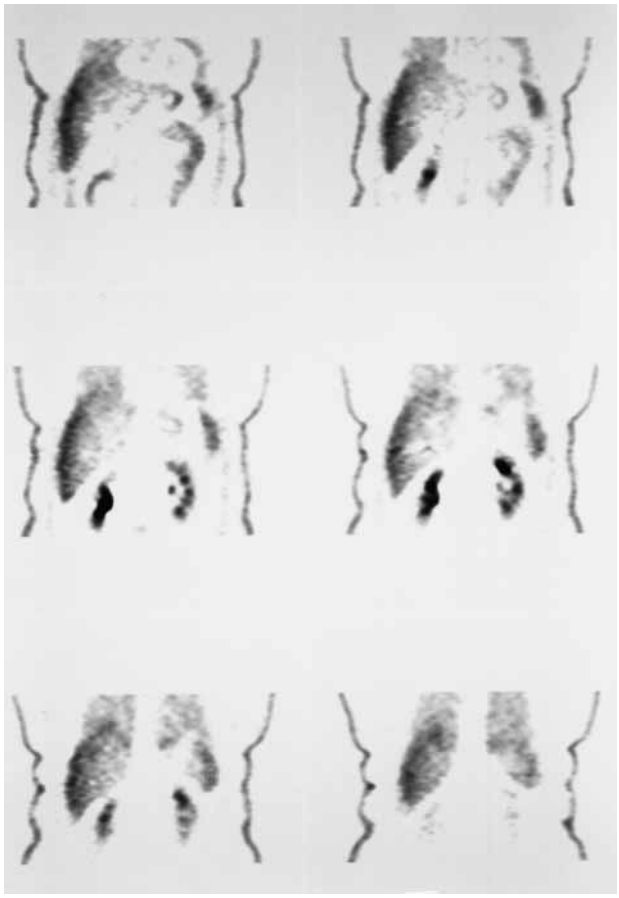

Fig. 1. 18F-FDG PET study of patient G.A. with histologically confirmed FNF of the liver (coronal orientation) showing no increased FDG uptake in segment IV/VII of the liver (SUV_{LBM}: 0.9).

reported in great detail. To our knowledge, there is only one published study in the literature reporting on 18F-FDG features of FNH with a very small number ($n=3$) of patients (7, 8). In the present study of eight histologically verified FNH, we describe the18F-FDG features of FNH, visually as well as (semi)quantitatively, using SUV and SUV_{LBM} (9).

Patients and methods

Eight patients (6 female, 2 male; mean age, 43.0±14.6 years, Table 1) with histologically confirmed FNH were prospectively investigated with 18F-FDG PET. All FNH lesions were incidental ultrasonographic findings. Two patients with melanoma and six patients with colorectal carcinoma having liver metastases served as controls (7 male, 1 female; mean age 72.1±4.0 years) All patients were imaged after fasting (except for water) for a minimum of 4–5 h. None of the patients had diabetes mellitus, and glucose serum levels were routinely measured before the administration of 18F-FDG.

Positron emission tomography

The 18F-FDG PET imaging was performed with a dedicated PET tomograph (GE Advance, GE Medical Systems, Wukesha, WI). The system yields 35 sections per FOV, axial slice thickness 4.25 mm. 18F-FDG was synthesized automatically using standard methods (FDG Microlab, GE Medical Systems).

Imaging protocol

After intravenous injection of 300–370 MBq 18F-FDG, a transmission scan was performed for 10 min per bed position, and a rotating germanium-68 rod source was used to create an attenuation map. The emission images were obtained for 10 min per bed position covering the liver region.

Image analysis

The images from PET studies were correlated with CT or MRI to provide an exact localization of the

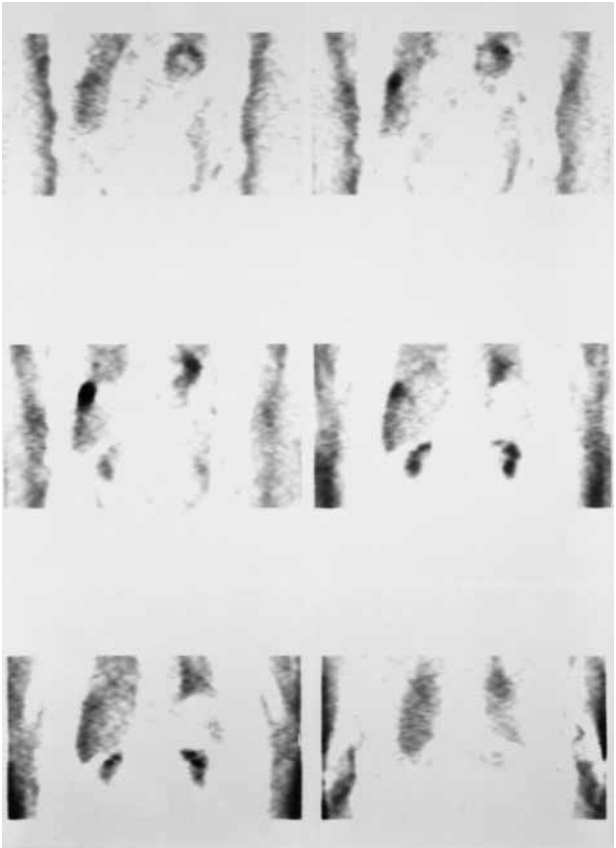

Fig. 2. 18F-FDG PET study of a patient (V.J.) with liver metastasis spread from colonic adenocarcinoma demonstrating a significantly increased FDG uptake (SUV_{LBM}:9.8).

lesion. The PET studies were interpreted visually, and the 18F-FDG accumulation of the lesions was scored as follows: (I) less, (II) equivocal, and (III) more than normal liver 18F-FDG uptake. The 18F-FDG images were additionally (semi)quantitated by using the standardized uptake value (SUV) after manually drawing the region of interest (ROI) around the lesions which were localized by radiological means (CT or MRI). These ROIs were drawn over areas of maximum activity within the lesion. The SUV was calculated as follows: SUV= activity in ROI in becquerels per milliliter/injected dose in becquerels per weight in kilograms (8). In addition, the SUV was corrected in all patients for LBM to avoid the overestimation of 18F-FDG uptake in heavy patients. LBM was calculated as $45.5+0.91\times$(patient height in cm minus 152) for women and $48.0+1.06\times91\times$(patient height in cm minus 152) for men (9). The ROI for the normal liver area was drawn over a tumor-free area. In one patient (H.E.) no SUV was available because of technical problems. All 18F-FDG images were read independently by two experienced nuclear medicine physicians (A.B., A.K.). The only information that the observers had was the localization of the lesion.

Table 1. Clinical data and PET findings for histologically confirmed FNH lesions

Patient	Sex	Age (years)	Lesion localization (CT/US/MRI): size (cm)	18F-FDG Uptake (score)	SUV	SUV_{LBM}
G.A	F	40	Segment VI/VII: 4.5 cm	I	1.5	0.9
E.S	F	34	Segment II/III : 5 cm	I	1.8	1.9
S.M	F	32	Segment VIII: 5 cm	I	2.1	2.1
P.E	F	46	Segment VII/VIII: 8.5 cm	II	2.5	1.8
H.E	M	59	Segment VI: 3 cm	II	n.a	n.a
M.U	F	59	Segment VII/VIII: 8 cm	II	2.6	2.1
G.E	F	28	Segment VI: 2.7 cm	I	2.1	1.7
W.J	M	50	Segments IV: 2 cm	II	2.3	2.2

Table 2. Clinical data and PET findings of liver metastases

Patient	Sex	Age (years)	Lesion localization (CT/US/MRI): size (cm)	18F-FDG Uptake (score)	SUV	SUV_{LBM}
S.F	M	69	Segment VIII: 3.7 cm	III	8.8	8.0
L.F	M	73	Segment VIII: 1.8 cm	III	6.9	5.6
P.A	F	75	Segment VI: 4.3 cm	III	6.7	5.9
F.J	M	79	Segment VII: 2 cm	III	16.0	14.2
F.R	M	69	Segment V: 3 cm	III	15.3	16.3
F.J	M	67	Segment IV: 6 cm	III	10.3	7.1
V.J	M	70	Segment VIII: 4 cm	III	10.4	9.8
K.F	M	75	Segment 4: 1.5 cm	III	6.2	6.3

Results

Patient data are summarized in Tables 1 and 2.

All liver metastases in the eight control patients were readily seen on PET images; visually, there was an increased (Score III) uptake of 18F-FDG. In two out of the eight patients, the 18F-FDG accumulation in the FNH lesion was graded as a Score I (25%), whereas in the remaining six patients (75%) the accumulation of 18F-FDG was indistinguishable from the surrounding normal liver tissue (Score II). None of FNH patients (0%) had a Score III. Consequently, (semi)quantitative assessment of 18F-FDG uptake revealed a significantly higher SUV for liver metastases (10.07 ± 3.79) as compared to the SUV of FNH lesions (2.12 ± 0.38). The SUV_{LBM} for liver metastases were (9.15 ± 4.03) also significantly higher than the SUV_{LBM} of FNH (1.81 ± 0.41) (Tables 1 and 2).

Discussion

In vivo studies of glucose metabolism using PET with 18F-FDG is a noninvasive technique clinically used to image a variety of malignant tumors (7, 8, 10), since most malignant tumor cells have an increased glucose metabolism and increased glycolysis. The reason for the 18F-FDG accumulation in malignant tumor cells is due to low levels of glucose-6-phosphatase (G-6-P), leading to intracellular trapping of 18F-FDG. 18F-FDG uptake is, however, not necessarily specific for malignant tumors, since inflammatory processes may also demonstrate an increased 18F-FDG uptake. The 18F-FDG accumulation in inflammatory lesions is probably due to activation of macrophages (8–11). It has been shown that, in normal human cells, the relative G-6-P concentration depends on the tissue type. While the myocardium and the brain contain lower G-6-P levels, the normal liver, for example, has high G-6-P activity. Consequently, the clearance of 18F-FDG from normal liver cells is relatively rapid, leading to absence of higher uptake of 18F-FDG in the liver. In contrast, the liver metastases can be readily detected on 18F-FDG images showing hot spots due to lower G-6-P concentration. In hepatocellular carcinomas (HCC) a varying degree of 18F-FDG accumulation has been described which is also related to the activity of G-6-P of the HCC cells, depending on the degree of tumor differentiation. That means that a well-differentiated HCC may be similar to normal hepatocytes. As a result, the 18F-FDG features of well-differentiated HCC and normal hepatocytes may also be similar, and 18F-FDG may fail to detect HCC (8, 9, 11). According to the literature,

30–50% of HCC demonstrate no 18F-FDG accumulation greater than the accumulation of the surrounding liver tissue (8). FNH of the liver is considered by some to be a tumor-like lesion (2) that is mostly discovered incidentally. It has been speculated that FNH is a reaction to a vascular anomaly. It contains hepatocytes, bile duct elements, Kupffer cells, and collagenous tissue. Despite advances in imaging modalities, the definite diagnosis of FNH may create a significant problem, especially in a cancer patient, if radiological imaging modalities are not diagnostic. With liver-specific MRI contrast agents, the differentiation between hepatocellular and non-hepatocellular tumors has become feasible in most patients because liver-specific MRI contrast agents tend to be taken up into hepatocellular tumors, including FNH (12, 13). However, It has been reported that an overlap may be present in the enhancement pattern between hypervascular malignant lesions and FNH and not all FNH may show the typical enhancement pattern on MRI studies, thus rendering a specific diagnosis difficult. A needle biopsy may, therefore, be necessary (1, 2, 6, 12, 13, 16). In our study, none of the FNH lesions showed high concentrations of 18F-FDG. This imaging finding of FNH by 18F-FDG PET appears to be in line with the histopathological structure of FNH. Hyperplastic, but non-neoplastic, hepatocytes, as in FNH, may cause an 18F-FDG accumulation comparable to that in normal hepatocytes. Therefore, it may speculated that FNH cells might contain lower levels of hexokinase activity and higher levels of G-6-P than normal liver cells (8–11, 14, 15).

In conclusion, our results indicate that FNH of the liver is not associated with a increased glucose metabolism and that the 18F-FDG accumulation in FNH is no higher than in normal liver tissue. An 18F-FDG study can not be considered as a baseline-screening method for differential diagnosis of focal liver lesions; however, it may be of clinical relevance in patients with known malignancy if other imaging modalities including MRI are not diagnostic.

Acknowledgments

The authors express their appreciation to I. Leitinger, G. Wagner, B. Wurzer, R. Bartosch, E. Bartosch, G. Icme, A. Krcal, H. Eidherr, and M. Mitterhauser, from the PET Center, University of Vienna, for their technical asistance.

References

1. Cherqui D, Rahmouni A, Charlotte F, et al. Management of focal nodular hyperplasia and hepatocellular adenoma in young women: A series of 41 patients with clinical, radiological, and pathological correlations. Hepatology 1995; 22: 1674–81.
2. Shirkhoda A, Farah M C, Bernacki I, et al. Hepatic focal nodular hyperplasia: CT and sonographic spectrum. Abdom Imaging 1994; 19: 34–8.
3. Nagorney D M. Benign hepatic tumours: Focal nodular hyperplasia and hepatocellular adenoma. World J Surg 1995; 19: 13–8.
4. Biersack H J, Thelen M, Torres J F, et al. Focal nodular hyperplasia of the liver as established by ^{99m}Tc-sulfur colloid and HIDA scintigraphy. Radiology 1980; 137: 187–90.
5. Calvet X, Pons F, Bruix J, et al. Technetium-99m-DIS-IDA hepatobiliary agent in diagnosis of hepatocellular carcinoma: relationship between detectability and tumour differentiation. J Nucl Med 1988; 29: 1916–20.
6. Kurtaran A, Müller C, Novacek, et al. Distinction between hepatic focal nodular hyperplasia and malignant liver lesions using technetium-99m-galactosyl-neoglycoalbumin. J Nucl Med 1997; 38: 1912–5.
7. Schiepers C, Hoh C K. Positron emission tomography as a diagnostic tool in oncology. Eur Radiol 1998; 8: 1481–94.
8. Delbeke D, Martin W H, Sandler M P, et al. Evaluation of benign vs malignant hepatic lesions with positron emission tomography. Arch Surg 1998; 133: 510–6.
9. Kim C K, Gupta N C. Dependency of standardized uptake values of fluorine-18 fluorodeoxyglucose on body size: Comparison of body surface area correction and lean body mass correction. Nucl Med Commun 1996; 17: 890–4.
10. Goldberg M A, Lee M J, Fischman A J, et al. Fluorodeoxyglucose PET of abdominal and neoplasms: Potential role in oncologic imaging. RadioGrafics 1993; 13: 1047–62.
11. Kubota R, Yamada S, Kubota K, et al. Nontumoral distribution of fluorine-18-fluorodeoxyglucose *in vivo*: high accumulation in macrophages and granulation tissues studied my microautoradiography. J Nucl Med 1992; 33: 1972–80.
12. Vogl T J, Hammerstingl R, Schwarz W, et al. Superparamagnetic iron oxide-enhanced versus gadolinium-enhanced MR imaging for differential diagnosis of focal liver lesions. Radiology 1996; 183: 881–7.
13. Coffin C M, Diche T, Mahmouz A, et al. Benign and malignant hepatocellular tumors; evaluation of tumor enhancement after mangafodipir trisodium injection on MR imaging. Eur Radiol 1999; 9: 444–9.
14. Weber G, Cantero A. Glucose-6-phosphatase activity in normal, precancerous, and neoplastic tissues. Cancer Res 1955; 15: 105–8.
15. Gallaghar B M, Fowler J S, Gutterson N I, et al. Metabolic trapping as a principle of radiopharmaceutical design: some factors responsible for the biodistribution of [18] 2-deoxy-2-fluoro-D-glucose. J Nucl Med 1978; 19: 1154–61.
16. Mahfouz A E, Hamm B, Taupitz M, Wolf K J. Hypervascular liver lesions: differentiation of focal nodular hyperplasia from malignant tumors with dynamic gadolinium-enhanced MR imaging. Radiology 1993; 186: 133–8.